Journal of Alloys and Compounds 500 (2010) 195–199

Contents lists available at ScienceDirect

Journal of Alloys and Compounds

journal homepage: www.elsevier.com/locate/jallcom

Microwave-assisted hydrothermal synthesis of Bi_2S_3 nanorods in flower-shaped bundles

Titipun Thongtem[a,*], Chalermchai Pilapong[a], Jutarat Kavinchan[a], Anukorn Phuruangrat[b,*], Somchai Thongtem[b]

[a] Department of Chemistry, Faculty of Science, Chiang Mai University, Chiang Mai 50200, Thailand
[b] Department of Physics and Materials Science, Faculty of Science, Chiang Mai University, Chiang Mai 50200, Thailand

ARTICLE INFO

Article history:
Received 18 January 2010
Received in revised form 22 March 2010
Accepted 31 March 2010
Available online 8 April 2010

Keywords:
Semiconductors
Chemical synthesis
Luminescence
Scanning electron microscopy
Transmission electron microscopy
X-ray diffraction

ABSTRACT

Bi_2S_3 nanorods in flower-shaped bundles were successfully synthesized from the decomposition of Bi–thiourea complexes under the microwave-assisted hydrothermal process. X-ray powder diffraction (XRD) patterns and field emission scanning electron microscopy (FE-SEM) show that Bi_2S_3 has the orthorhombic phase and appears as nanorods in flower-shaped bundles. A transmission electron microscopic (TEM) study reveals the independent single Bi_2S_3 nanorods with their growth along the [0 0 1] direction. A possible formation mechanism of Bi_2S_3 nanorods in flower-shaped bundles is also proposed and discussed. Their UV–vis spectrum shows the absorbance at 596 nm, with its direct energy band gap of 1.82 eV.

1. Introduction

In recent years, the fabrication of nanomaterials and nanodevices has been widely and deeply researched due to the novel properties comparing to their normal counterparts, and strong dependence on their characteristics such as shape, size and crystallinity [1,2]. Among them, one-dimensional (1D) nanostructures possess unique physical, chemical, and electron-transport properties, different from those of bulky and isotropic materials [2–4].

Binary metal chalcogenides of $A_2^{V}X_3^{VI}$ (A = As, Sb, Bi; X = S, Se, Te) semiconductors have a number of applications including photoconducting targets of television cameras, electronic and optoelectronic devices, thermoelectric devices, and infrared (IR) spectroscopy [2,4–6]. Bismuth sulfide (Bi_2S_3) has a 1.3 eV direct band gap, and is suitable for application in photovoltaic materials, photodiode arrays, sensors and IR spectroscopy photovoltaic converters, thermoelectric cooling technologies based on the Peltier effect [2,3,5,7–10]. The convention hydrothermal (CH) method has been widely used to synthesize the Bi_2S_3 nanomaterials [1–7]. It was able to control the morphologies: nanorods, nanowires, agglomerated particles and urchinlike [1–8].

Herein, an economical method to synthesize Bi_2S_3 nanorods in flower-shaped bundles by microwave-assisted hydrothermal (MH) method is reported. This method is simple, fast and inexpensive, as compared to the convention hydrothermal (CH) one.

2. Experimental procedure

The analytical grade chemicals: bismuth nitrate pentahydrate ($Bi(NO_3)_3{\cdot}5H_2O$), thiourea (NH_2CSNH_2) and polyvinylpyrrolidone (PVP) were used without further purification. To synthesize Bi_2S_3 flower-like structure, 0.005 mole $Bi(NO_3)_3{\cdot}5H_2O$ and 0.001 mole NH_2CSNH_2 were dissolved in 60 ml distilled water, and followed by 0.5 ml 37% HNO_3 and 0.5 g PVP adding, respectively. The mixture was stirred for 30 min at room temperature and put into a 100 ml Teflon-lined autoclave, which was tightly closed, heated up to 200 °C by a 300 W microwave radiation, held at this temperature for 1 h, and then naturally cooled to room temperature. After the microwave-assisted hydrothermal process, the product was filtered, washed with distilled water and absolute ethanol for several times, and dried at 80 °C for 24 h. This process was also repeated by using the convention hydrothermal method, heated by an electric oven, at 200 °C for 24 h.

The products were analyzed using an X-ray diffractometer (D8 Advance, Bruker Ltd., Germany) with Cu Kα radiation in the 2θ range from 5° to 80°. The Raman spectra was recorded on HORIBA JOBIN YVON T64000 Raman spectrometer using 50 mW Ar Laser with $\lambda = 514.5$ nm. The morphology of the product was characterized by a JSM-6335F scanning electron microscope (SEM, JEOL Ltd., Japan) and JEM-2010 transmission electron microscope (TEM, JEOL Ltd., Japan). The room temperature UV–vis spectrum was collected on a UV/VIS spectrometer PerkinElmer LAMBDA 40 at wavelength range of 200–1300 nm with the scanning rate of 0.5 nm s^{-1}.

* Corresponding authors. Tel.: +66 53 943344; fax: +66 53 892277.
E-mail addresses: ttpthongtem@yahoo.com (T. Thongtem), phuruangrat@hotmail.com (A. Phuruangrat).

0925-8388/$ – see front matter © 2010 Elsevier B.V. All rights reserved.
doi:10.1016/j.jallcom.2010.03.240

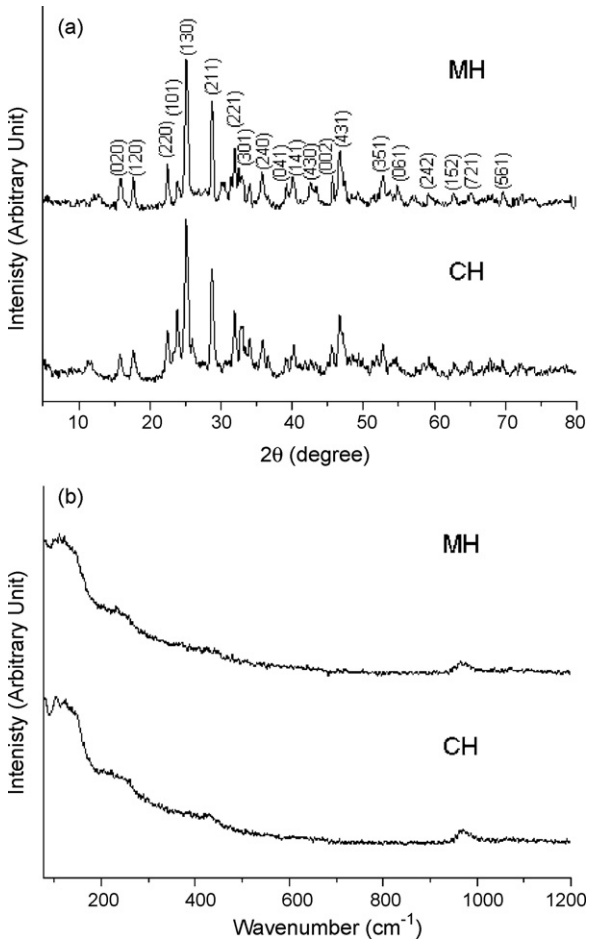

Fig. 1. (a) XRD patterns and (b) Raman spectra of Bi_2S_3 synthesized by the conventional hydrothermal and microwave-assisted hydrothermal methods.

3. Results and discussion

Fig. 1a shows the XRD patterns of the products synthesized by the MH and CH methods. All diffraction peaks match very well with the Bi_2S_3 JCPDS no. 17-0320 [11] with no detection of any impurities. The XRD intensity synthesized by the MH is higher than that synthesized by the CH. It implies that Bi_2S_3 synthesized by the first is better crystalline than Bi_2S_3 synthesized by the second. All the diffraction peaks of the Bi_2S_3 nanorods in flower-shaped bundles were shifted towards the lower angles, as compared to the JCPDS database, caused by an increase in their interplanar spaces. This may be attributed to the existence of the stress in the lattice of Bi_2S_3 nanorods in flower-shaped bundles. EDX spectrum of Bi_2S_3 produced by the MH method (un-shown result) detected only Bi and S peaks, in accordance with its constituents. Quantitative EDX analysis showed that the atomic ratio of Bi:S is 38:62, very close to the composition of Bi_2S_3. A definite existence of Bi_2S_3 was analyzed using a Raman spectrometer as shown in Fig. 1b. The spectra show four vibration modes, at 139.6, 253.7, 310.0 and 968.9 cm^{-1}. The first is in accordance with the 139.4 cm^{-1} mode of Bi_2S_3 nanorods, specified as the surface phonon vibration [12]. The second corresponds with the vibration mode of Bi_2S_3 nanorods at 252.0 and 259 cm^{-1} [12,13] and Bi_2S_3 nanoribbons and hierarchical nanostructures at 250 cm^{-1}, specified as the vibration mode of Bi–S bonds [14,15]. The detections of the third and fourth were in accordance with those of Bi_2S_3 nanorods at 312 and 975 cm^{-1} [13]. In the FTIR spectrum of PVP, it shows the wave numbers at 3450, 2930, 1675, 1420 and 1290 cm^{-1} – assigned to be the OH stretching vibration, CH_2 unsymmetrical stretching vibration, CO stretching vibration, CH_2 bending vibration and CN stretching vibration, respectively [16,17]. There was no detection of these impurity peaks in the FTIR spectrum of Bi_2S_3 (un-shown result), which implied that the product was pure phase.

SEM images of Bi_2S_3, prepared by the MH and CH methods, are given in Fig. 2. Only Bi_2S_3 irregular crystalline (Fig. 2a) with the average size of 1.5 μm was synthesized by the CH process. These nanorods agglomerate together to form clusters, and are not separate as independent nanorod bundles. Comparing to the synthesis of large-scale single-crystalline Bi_2S_3 nanowires by a simple one-step hydrothermal reaction of $Bi(NO_3)_3{\cdot}5H_2O$ and $Na_2S_2O_3$ at 180 °C for 2 days, the product contained a large quantity of nanowires with their lengths of hundreds of nanometers to a few microns range [18]. When microwave radiation was used as the heating source, the clearly independent Bi_2S_3 nanorods in flower-shaped bundles were detected. The use of microwave radiation as heating source shows the formation of uniform and perfect Bi_2S_3 flower-like bundles with the approximate diameter of 3–4 μm including the approximate length of the nanorods of 1–2 μm. The anisotropic growth of the Bi_2S_3 crystallites was further confirmed by the TEM analysis.

Fig. 3 shows TEM images of Bi_2S_3 nanorods in flower-shaped bundles synthesized by the MH method. The Bi_2S_3 flowers of Fig. 3a and b are composed of more than a hundred of individual Bi_2S_3 nanorods grow from the Bi_2S_3 cores. It is obvious that the morphology of Bi_2S_3 nanorods in flower-shaped bundles with 3–5.5 μm in size is in accordance with the SEM image (Fig. 2b) shown above. Fig. 3c shows the broken Bi_2S_3 nanorods form the Bi_2S_3 flower-like cores. The length of the individual nanorod of Bi_2S_3 is approximately 500–1500 nm. The growth direction of Bi_2S_3 nanorods in flower-shaped bundles was studied using high resolution trans-

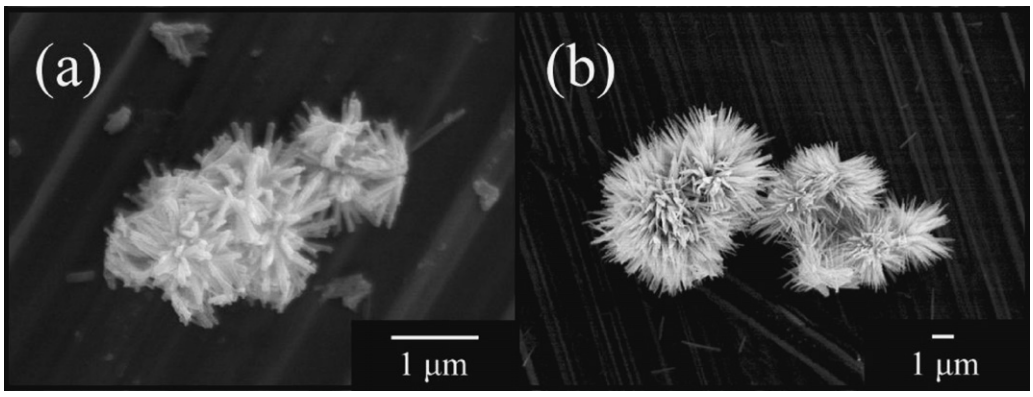

Fig. 2. SEM images of Bi_2S_3 nanorods in bundles synthesized by the (a) conventional hydrothermal and (b) microwave-assisted hydrothermal methods.

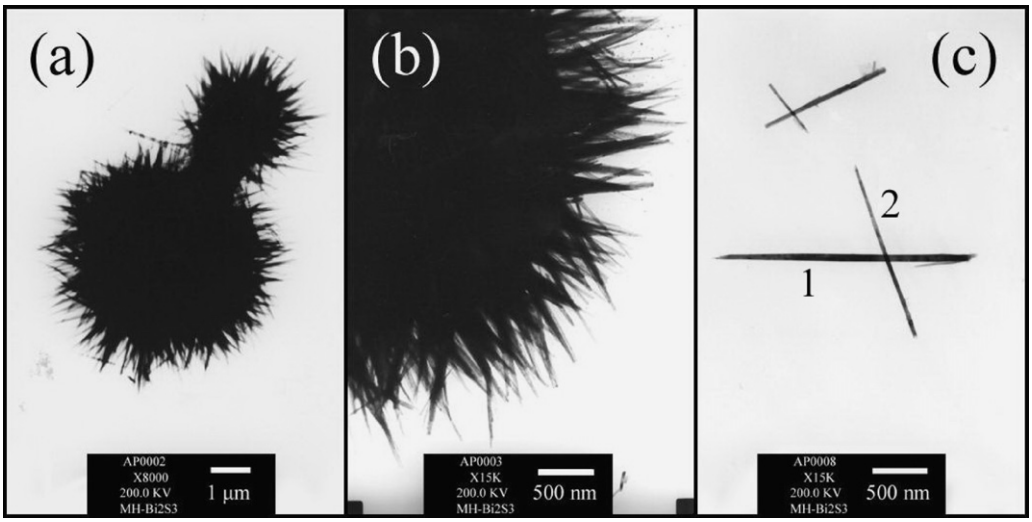

Fig. 3. TEM images of Bi_2S_3 nanorods in flower-shaped bundles synthesized by the MH method at (a) low and (b) high magnifications. (c) The broken nanorods from the flower-like cores.

mission electron microscopy (HRTEM) and selected area electron diffraction (SAED). They were characterized on areas 1 and 2 of TEM image (Fig. 3c). HRTEM images of Fig. 4a and c show lattice fringes of crystallographic planes with 3.96 Å space in parallel with the nanorods, corresponding to the (2 2 0) planes of orthorhombic Bi_2S_3 phase. The HRTEM images demonstrate that the Bi_2S_3 nanorods synthesized by the MH and CH methods grow along the [0 0 1] direction – in accordance with the growth direction of Bi_2S_3 nanorods and nanowires characterized by other researchers [1,3,19]. Both SAED patterns in areas 1 and 2 appear as bright spots composing electron diffraction patterns (Fig. 4b and d), revealing that individual Bi_2S_3 nanorods broken from flower-like cores are single crystal Bi_2S_3 with high degree of crystallinity. The SAED patterns can be indexed as the orthorhombic phase of Bi_2S_3 (JCPDS

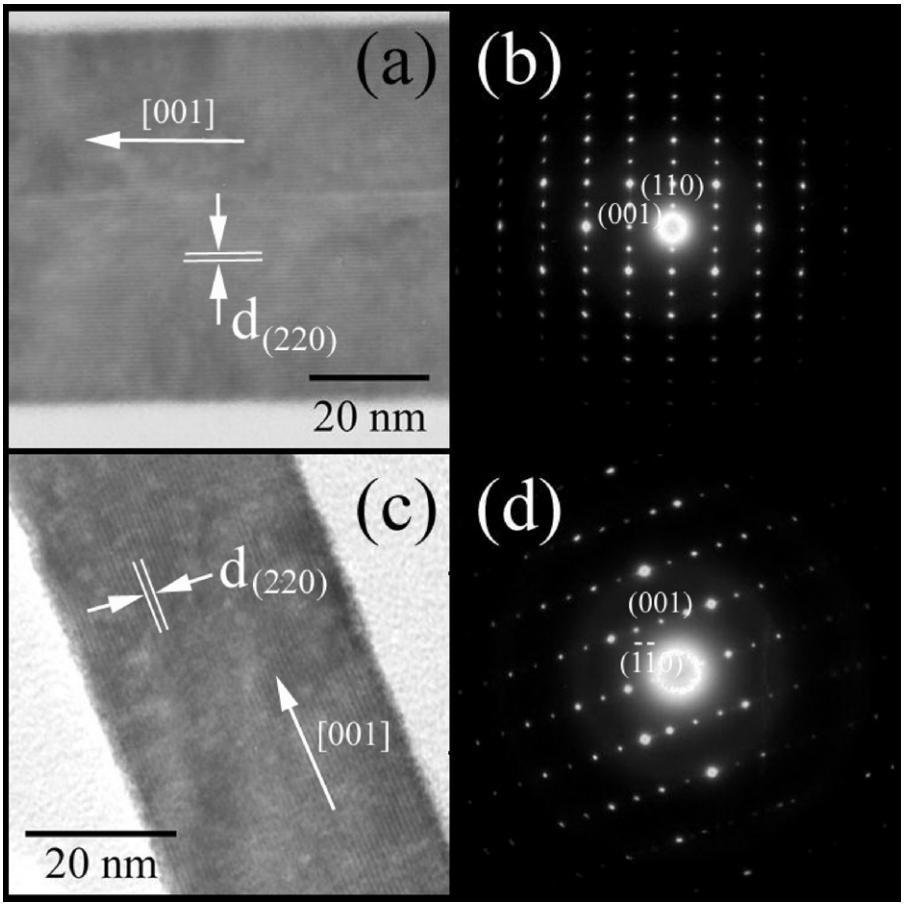

Fig. 4. HRTEM images and SAED patterns of Bi_2S_3 nanorods in bundles synthesized by the (a and b) conventional hydrothermal, and (c and d) microwave-assisted hydrothermal methods.

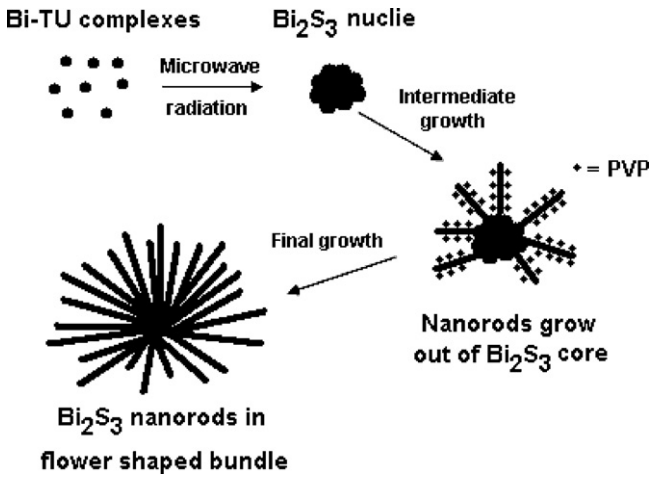

Fig. 5. Schematic illustration for the formation mechanism of Bi_2S_3 nanorods in flower-shaped bundles.

no. 17-0320) with the same [$\bar{1}$ 1 0] zone axes, which further confirm that the structure of the nanorods is orthorhombic phase, in accordance with the XRD analysis.

The formation mechanism of Bi_2S_3 nanorods in flower-shaped bundles is schematically shown in Fig. 5. First, the strong complex action between Bi^{3+} and thiourea (TU) leads to the formation of Bi–TU complexes [9]. For NH_2CSNH_2 compound, it has pair electrons on nitrogen and sulfur atoms, which have the great coordinating ability with inorganic metal cations, such as Cd^{2+}, Cu^{2+} and Pb^{2+} to form the metal–thiourea complexes [20]. Under microwave-assisted hydrothermal process, the Bi–TU complexes decomposed and formed the Bi_2S_3 nuclei. Then the Bi_2S_3 nanorods grew on the surface of Bi_2S_3 nuclei to form Bi_2S_3 nanorods in flower-shaped bundles. The formation reactions may be described as follows.

$$Bi^{3+} + TU \rightarrow \text{Bi–TU complexes} \quad (1)$$

$$\text{Bi–TU complexes} \rightarrow Bi_2S_3 \quad (2)$$

The growth process of Bi_2S_3 nanorods in flower-shaped bundles contains mainly two stages – the nucleation and crystal growth. For the present research, $Bi(NO_3)_3$ reacts with TU to form Bi–TU complexes at the initial stage. At the intermediate stage, the Bi–TU complexes decomposed to produce Bi_2S_3 nuclei by the microwave-assisted hydrothermal process. At this stage, PVP adsorbed on Bi_2S_3 nuclei – leading to the Bi_2S_3 nucleation as seeds which act as initial nuclei for particle growth. When the particles reach the critical dimension, PVP absorbed on the small particles by the side linked Bi_2S_3 units forming infinite chains parallel to the *c*-axis acting as a template for the formation of Bi_2S_3 nanorods in flower-shaped bundles. The final stage is the Bi_2S_3 nanorods in flower-shaped bundles, obtained by a novel microwave hydrothermal method, - homogeneous in size and form much similar to a flower with thorns found in nature [9,10,21]. In general, the growth of 1D Bi_2S_3 nanomaterials is a preferential growth direction along the *c*-axis due to the difference bonding in Bi_2S_3 structure. Bi_2S_3 is a lamellar structure with linked Bi_2S_3 units forming infinite chains parallel to the *c*-axis. The stronger covalent bond between the planes perpendicular to the *c*-axis supports higher growth rate along the *c*-axis. The much weaker van der Waals bonding between the planes perpendicular to the *a*-axis limits the growth of the fibers in the horizontal direction and supports their cleavage to form one-dimensional nanostructure [22].

The optical property of the product was investigated by UV–vis spectroscopy. Fig. 6 presents the UV–vis absorbance spectrum, and $(\alpha h\nu)^2$ vs. $h\nu$ curve of Bi_2S_3 nanorods in flower-shaped bundles synthesized by the MH method. The UV–vis spectrum showed the blue shifted absorption at 596 nm as compared to the 953 nm absorption for bulk Bi_2S_3 [23]. It can be attributed to the excitonic absorbance due to the quantum confinement at low dimension compared to its bulk counterparts [23]. The direct band gap of the product was calculated from its optical absorption spectrum by plotting $(\alpha h\nu)^2$ vs. $h\nu$ curve where α is the absorbance, h the Planck constant and ν the frequency [24] is shown in Fig. 6b. The direct band gap (E_g) of the Bi_2S_3 semiconducting nanorods in flower-shaped bundles was determined to be at 1.82 eV. This value is in good agreement with the 1.85 eV band gap of Bi_2S_3 nanowires [22], and 1.8 eV band gap of Bi_2S_3 thin films [24].

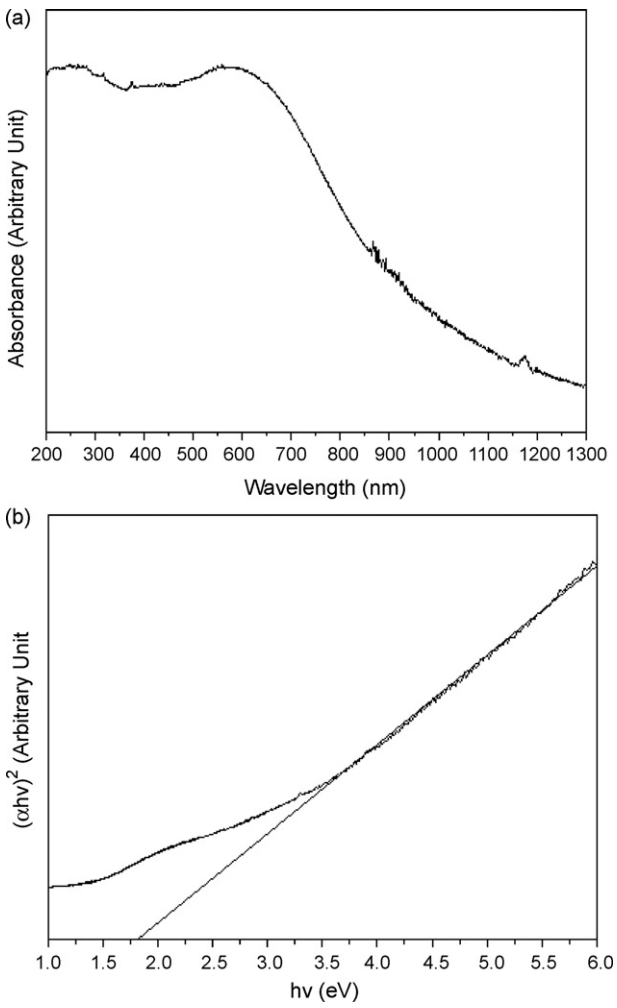

Fig. 6. (a) UV–vis absorbance, and (b) $(\alpha h\nu)^2$ vs. $h\nu$ curve of Bi_2S_3 nanorods in flower-shaped bundles synthesized by the microwave-assisted hydrothermal method.

4. Conclusions

Microwave-assisted hydrothermal reaction has emerged as an alternative route of fine powder synthesis. It was demonstrated that this simple method can be used to synthesize Bi_2S_3 nanostructure. XRD, SEM and TEM analyses proved that the product is orthorhombic Bi_2S_3 nanorods in flower-shaped bundles with the size of 3–5.5 μm. The microwave-assisted hydrothermal process for the synthesis of nanomaterials is shown to be very effective, inexpensive, short reaction time and environmentally benign. The direct energy band gap of the product was determined to be 1.82 eV – in agreement with those of other researchers.

Acknowledgements

This research was supported by the National Nanotechnology Center (NANOTEC), a member of National Science and Technology Development Agency (NSTDA), Ministry of Science and Technology, and the Thailand Research Fund, Bangkok, Thailand.

References

[1] Z.J. Zhang, X.Y. Chen, J. Phys. Chem. Solids 70 (2009) 1121–1131.
[2] L. Tian, H.Y. Tan, J.J. Vittal, Cryst. Growth Des. 8 (2008) 734–738.
[3] C.J. Tang, G.Z. Wang, H.Q. Wang, Y.X. Zhang, G.H. Li, Mater. Lett. 62 (2008) 3663–3665.
[4] Q. Han, J. Chen, X. Yang, L. Lu, X. Wang, J. Phys. Chem. C 111 (2007) 14072–14077.
[5] J. Lu, Q. Han, X. Yang, L. Lu, X. Wang, Mater. Lett. 61 (2007) 3425–3428.
[6] G. Xie, Z.P. Qiao, M.H. Zeng, X.M. Chen, S.L. Gao, Cryst. Growth Des. 4 (2004) 513–516.
[7] X. Zhu, J. Ma, Y. Wang, J. Tao, B. Lin, Y. Ren, X. Jiang, J. Liu, Ceram. Int. 34 (2008) 249–251.
[8] Y. Jiang, Y.J. Zhu, Z.L. Xu, Mater. Lett. 60 (2006) 2294–2298.
[9] A. Phuruangrat, T. Thongtem, S. Thongtem, Mater. Lett. 63 (2009) 1496–1498.
[10] T. Thongtem, A. Phuruangrat, S. Wannapop, S. Thongtem, Mater. Lett. 64 (2010) 122–124.
[11] Powder Diffract. File, JCPDS-ICDD, Newtown Square, PA, USA, 2001.
[12] X. Yang, X. Wang, Z. Zhang, Mater. Chem. Phys. 95 (2006) 154–157.
[13] J. Ota, S.K. Srivastava, J. Phys. Chem. C 111 (2007) 12260–12264.
[14] Y. Sun, Q. Han, J. Lu, X. Yang, L. Lu, X. Wang, Mater. Lett. 62 (2008) 3730–3732.
[15] Q. Han, Y. Sun, X. Wang, L. Chen, X. Yang, L. Lu, J. Alloys Compd. 481 (2009) 520–525.
[16] X. Sui, Y. Liu, C. Shao, Y. Liu, C. Xu, Chem. Phys. Lett. 424 (2006) 340–344.
[17] T.T. Tseng, W.J. Tseng, Ceram. Int. 35 (2009) 2837–2844.
[18] Y. Yu, W.T. Sun, Mater. Lett. 63 (2009) 1917–1920.
[19] Y. Yu, C.H. Jin, R.H. Wang, Q. Chen, L.M. Peng, J. Phys. Chem. B 109 (2005) 18772–18776.
[20] S.H. Yu, J. Yang, Z.H. Han, Y. Zhou, R.Y. Yang, Y.T. Qian, Y.H. Zhang, J. Mater. Chem. 9 (1999) 1283–1287.
[21] D.P. Volanti, D. Keyson, L.S. Cavalcante, A.Z. Simões, M.R. Joya, E. Longo, J.A. Varela, P.S. Pizani, A.G. Souza, J. Alloys Compd. 459 (2008) 537–542.
[22] W. Li, Mater. Lett. 62 (2008) 243–245.
[23] M. Salavati-Niasari, D. Ghanbari, F. Davar, J. Alloys Compd. 488 (2009) 442–447.
[24] V.V. Killedar, S.N. Katore, C.H. Bhosale, Mater. Chem. Phys. 64 (2000) 166–169.